REGULAR ARTICLE

Effect of substituents at the heteroatom on the structure and ligating properties of carbodicarbenes and its silicon analogs: a theoretical study

Ankur Kanti Guha · Bidisha Konwar · Satyajit Sarmah · Ashwini K. Phukan

Abstract Density functional calculations have been carried out to investigate the effect of substituents attached to the heteroatoms of *N*-heterocyclic carbenes (NHCs) on the structure and ligating properties of carbon(0) [C(NHC)$_2$] and silicon(0) [Si(NHC)$_2$] compounds. The substituents were found to have a profound role on the structure and ligating properties of these classes of compounds. Fluoro- and chloro-substituted carbon(0) compounds were found to have quasi-linear geometries in which their C(0) characteristics are "masked." However, their C(0) characteristics become prominent in their protonated species. Large negative charges and shallow bending potential of the central C_c–C_0–C_c angle provide evidence for the "hidden C(0) characteristics" of these two compounds. Electron withdrawing substituents at N-atoms of the two NHCs dramatically decreases the basicity of these compounds. Both natural bonding and atoms in molecules analysis suggest that the most favorable Lewis structure of C(NHC)$_2$ and Si(NHC)$_2$ in their equilibrium geometries should be described (portrayed) as L=C=L and L → Si ← L, respectively, where L = NHCs.

A. K. Guha · B. Konwar · S. Sarmah · A. K. Phukan (✉)
Department of Chemical Sciences, Tezpur University,
Napaam, Tezpur, Assam 784028, India
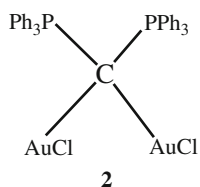e-mail: ashwini@tezu.ernet.in

1 Introduction

Carbon, the basic element of life, is usually found in tetrahedral form in organic compounds where all four valence electrons of the carbon atom are involved. However, the isolation of a stable singlet *N*-heterocyclic carbene (NHC) in 1991 had established the presence of another stable form of carbon where only two electrons are involved in bonding and the remaining two electrons form a lone pair [1–3]. Although it seems unrealistic for carbon compounds to have carbon atom with two orthogonal lone pairs, examples of such carbogenic compounds are now available in the literature [4–9]. Carbodiphophorane **1**, (Fig. 1) was synthesized way back in 1961 by Ramírez [4] and structurally characterized by an X-ray analysis in 1978 [5].

The resonance extreme **C** that suggests the presence of two lone pairs at the central carbon atom was also proposed [4–6, 10], but unsuccessful isolation of any geminal dimetalated derivative of **1** posed a question on the existence of the resonance extreme **C**. However, in 2002, Vicente et al. [11, 12], in a carefully designed experimental work, reported the isolation and characterization of the first geminal dimetalated derivative of **1**. The successful isolation of **2**, the dimetalated derivative of **1,** clearly demonstrated the dominant contribution of the resonance extreme **C** (Scheme 1) in describing the reactivity of **1**.

2

In an effort to understand the actual nature of bonding in **1** and related compounds, Frenking et al. and others carried out a series of systematic study and concluded that the bond between the central carbon atom and the two donor ligands L is of donor–acceptor type, L → C←L (where L can be any donor moiety) [13–20]. This bonding situation results in the retention of two lone pairs, one having σ symmetry and the other having π symmetry at the central carbon atom. In another report, Frenking et al. theoretically predicted that the compound $C(NHC)_2$ (**3**) (NHC = N-heterocyclic carbene) exhibits the characteristics of divalent C(0) compounds and could be isolable [20]. Experimental verification of this theoretical prediction came soon after when the group of Bertrand [8] synthesized a benzannulated derivative of **3** (Scheme 1).

Although experimental structural details of tetrakis(dimethylamino)allene, **4** is not available in the literature, its existence and isolation has been reported [21–24].
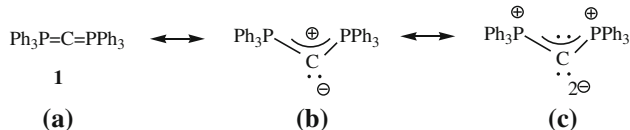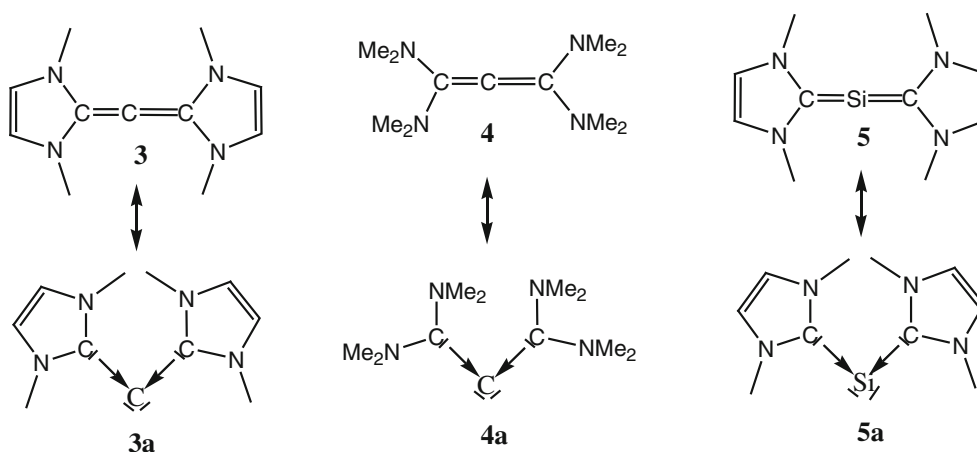

Fig. 1 Possible resonance forms of **1** showing the presence of two lone pairs at the central carbon atom

Frenking et al. have predicted that both allene $H_2C=C=CH_2$ and tetrakis(dimethylamino)allene $(Me_2N)_2C=C=C(NMe_2)_2$ are linear species [15, 16], but, tetrakis(dimethylamino)allene $(Et_2N)_2C=C=C(NEt_2)_2$ is bent with a C=C=C angle of 169° [14]. They also predicted that the bonding situation in tetraaminoallenes (TAAs) is of donor–acceptor type rather than an allenic one [14, 15]. This donor–acceptor bonding situation dominates their chemical properties. Specifically, TAAs forms stable dipolar adducts with CO_2, CS_2, or SO_2 [21] and reacts with metal templates such as $[(Ph_3P)Au]^+$ to give the structurally unusual η^1-adduct rather than the η^2-bound π-complex, as expected for a normal allene ligand [9]. Further, the crystal structure of a diprotonated species of $(H_2N)_2C=C=C(NH_2)_2$ proves the C(0) character of TAAs [25]. Thus, it is seen that substituents attached to the nitrogen atoms of the amino groups in TAAs has a dramatic role to play in dictating their equilibrium geometries (linear or bent) [26].

The chemistry of divalent element(0) is not limited only to carbon. Heavier homologs of carbon also exhibit typical chemistry of divalent carbon(0) compound. In a theoretical report, Frenking et al. suggested that the experimentally known "trisilaallene" [27] could be better considered as a divalent silicon(0) compound [28]. In the same report, they had shown that the compound $Si(NHC)_2$ (**5**) can also be considered as divalent Si(0) compound.

Since the electronic as well as ligating properties of NHCs can be tuned by putting different substituents at the heteroatom [2, 3, 29], therefore, it seems reasonable that substituents attached to the N-atoms of the two NHCs in $C(NHC)_2$ and $Si(NHC)_2$ are likely to affect the electronic as well as ligating properties of $C(NHC)_2$ and $Si(NHC)_2$. We report here a systematic analysis on the effect of substituents (R in Scheme 2) at the heteroatoms of the two
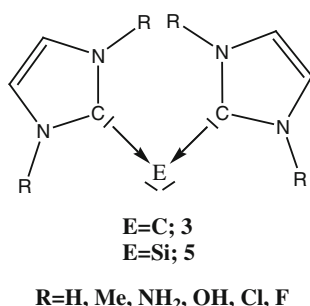

Scheme 1 Carbodicarbene, $(NHC)_2C$ (**3**), tetrakis(dimethylamino)allene, (**4**) and silicon analog of carbodicarbene, $(NHC)_2Si$ (**5**). The resonance extremes of these species (**3a–5a**), which describe their element(0) properties are also shown

E=C; 3
E=Si; 5

R=H, Me, NH$_2$, OH, Cl, F

Scheme 2 Schematic representation of (NHC)2C (3) and (NHC)2Si (4) with different substituents (R)

NHCs on the structure and ligating properties of C(NHC)$_2$ and Si(NHC)$_2$, respectively.

2 Computational details

All the structures were fully optimized without any symmetry constraint using density functional theory at BP86 level of theory [30, 31]. Triple zeta polarization (TZVP) [32] basis set were used for all the elements. Frequency calculations were performed at the same level of theory to characterize the nature of the stationary points. All the structures were verified as minimum on the potential energy surface by confirming that all the frequencies are real. Proton affinities are calculated with zero point energy corrections only. The bonding nature of these molecules was analyzed using natural bond orbital (NBO) analysis [33–35]. All these calculations were performed using Gaussian 03 suite of program [36]. Further, to analyze the bonding situation in **3** and **5**, we have carried out quantum theory of atoms in molecules (QTAIM) analysis using Bader's theory of atoms in molecules [37, 38]. QTAIM analyses were performed using AIMALL suite of program [39].

3 Results and discussion

3.1 Molecular geometry

The optimized geometries of the parent carbodicarbenes are given in Fig. 2, and the geometrical parameters of the same have been tabulated in Table S1, supporting information.

All the optimized geometries of the divalent C(0) compound, C(NHC)$_2$ are bent at the central carbon atom ($<C_c$–C_0–C_c = 125.9–131.9°) except for **3F** and **3Cl** ($<C_c$–C_0–C_c = 174.7° and 174.5° for **3Cl** and **3F,** respectively), which attain a quasi-linear geometry around the central carbon atom (Fig. 2). The two NHCs attached to the central carbon

atom of **3H**–**3OH** are in a twisted form making an angle with the central C–C–C plane that ranges from 29.9 (**3H**) to 36.9° (**3Me**). For **3H** to **3OH**, the substituents attached to the N-atoms of the two NHCs are in the plane of the NHC framework (Fig. 2). On the other hand, in **3F** and **3Cl**, the two NHCs are perpendicular to each other, and the F and Cl atoms are in a *syn* arrangement with the two NHCs. It had been noted by Frenking et al. that the C_0–C_c bond becomes stronger when the two NHCs are in a perpendicular arrangement [15].

It is evident from Fig. 2 that replacement of the substituents attached to the two heteroatoms of the NHC ligands dramatically changes the C_c–C_0 bond lengths. The bond length decreases from **3H** through **3F** as the pure σ donating H and Me groups are replaced by more electronegative π donating groups. The shortest C_c–C_0 distance is computed for **3F,** which is even shorter than the C–C distance in ethylene (1.32 Å). It is seen that the N–C_c distance is more in carbodicarbene than in the free carbenes (Table S1). The difference in the values of r_{N-Cc} steadily increases from **3H** (Δr_{N-Cc} = 0.03 Å) through **3F** (Δr_{N-Cc} = 0.10 Å). It can also be seen from Table S1 that corresponding to an increase in the values of r_{N-Cc} in carbodicarbene, the r_{C0-Cc} value decreases. These structural changes can be understood by looking at Scheme 3. In the free carbene, the N–C_c bonds develop partial double-bond character that results from interaction between the filled lone pair (LP) orbital at N and the formally vacant p_π orbital at C_c (Scheme 3a). However, in carbodicarbenes, both the filled lone pair orbitals at nitrogen and the central carbon atom compete for the vacant orbital at C_c (Scheme 3b). By virtue of similar electronegativity, the filled lone pair orbital at C_0 is closer in energy to the vacant p_π orbital centered at C_c, and thus, this interaction dominates (Scheme 3c) resulting in the formation of a partial C_c–C_0 double bond. Pi donating substituents attached to the N-atoms of the two NHCs lowers the energy of the formally vacant p_π orbital of C_c resulting in a stronger C_0–C_c interaction. Figure 3 displays the correlation between the energy of the formally vacant p_π orbital (E_{LUMO}) of the free carbene and the C_0–C_c distance. Lower is the value of E_{LUMO}, shorter, and hence, stronger will be the C_0–C_c bond.

The charge at the central carbon atom (C_0) also varies on changing the substituents. In case of **3H** through **3OH**, negative charge is obtained at the C_0 atom. These negative charges are consistent with the donor–acceptor interaction, NHC → C ← NHC. However, for **3F** and **3Cl**, charge at C_0 becomes positive, which might be due to attainment of quasi-linear geometry around the central carbon atom. The quasi-linear geometries of **3F** and **3Cl** as well as the positive natural charges at the central carbon atom raise an important question—"Do these two compounds really
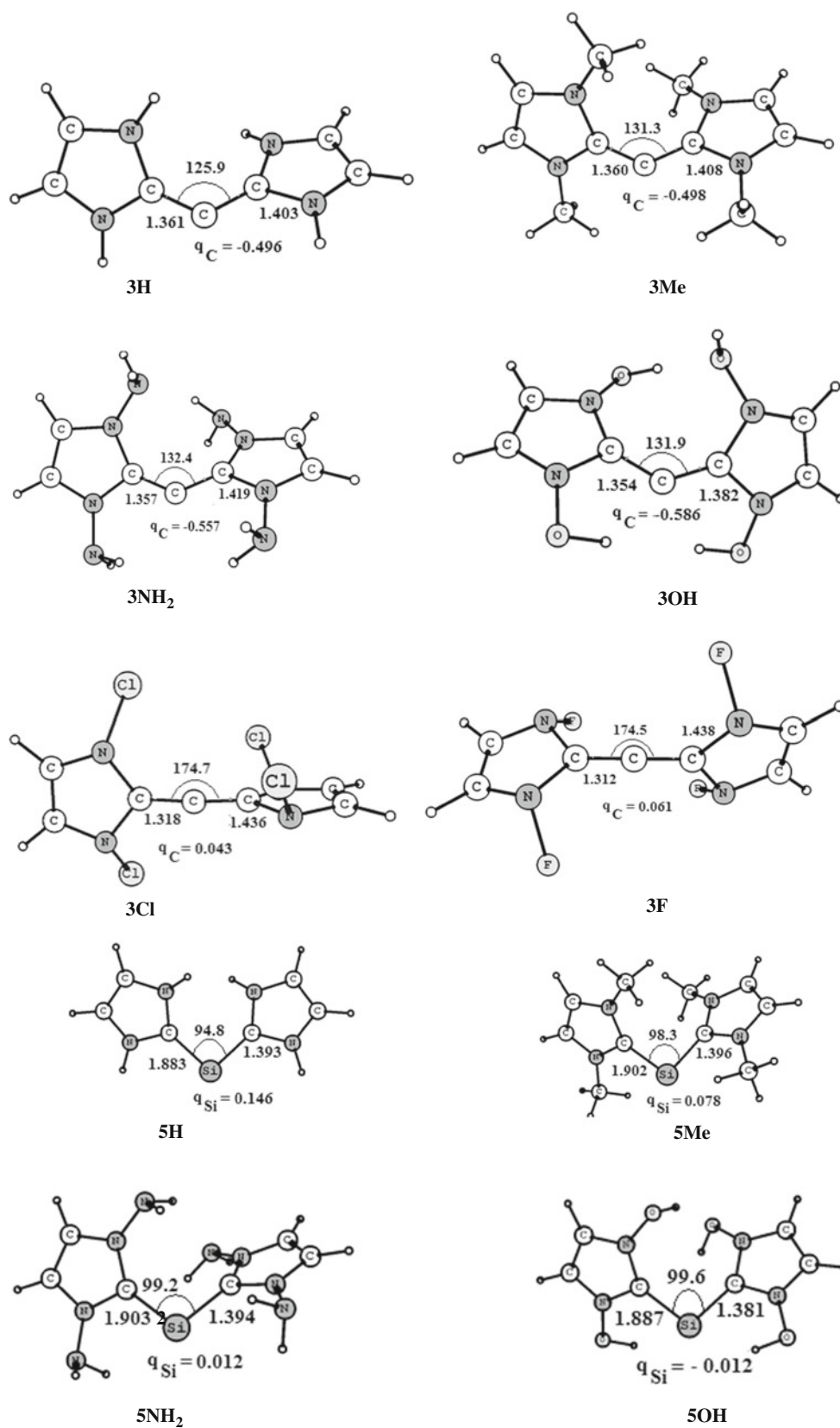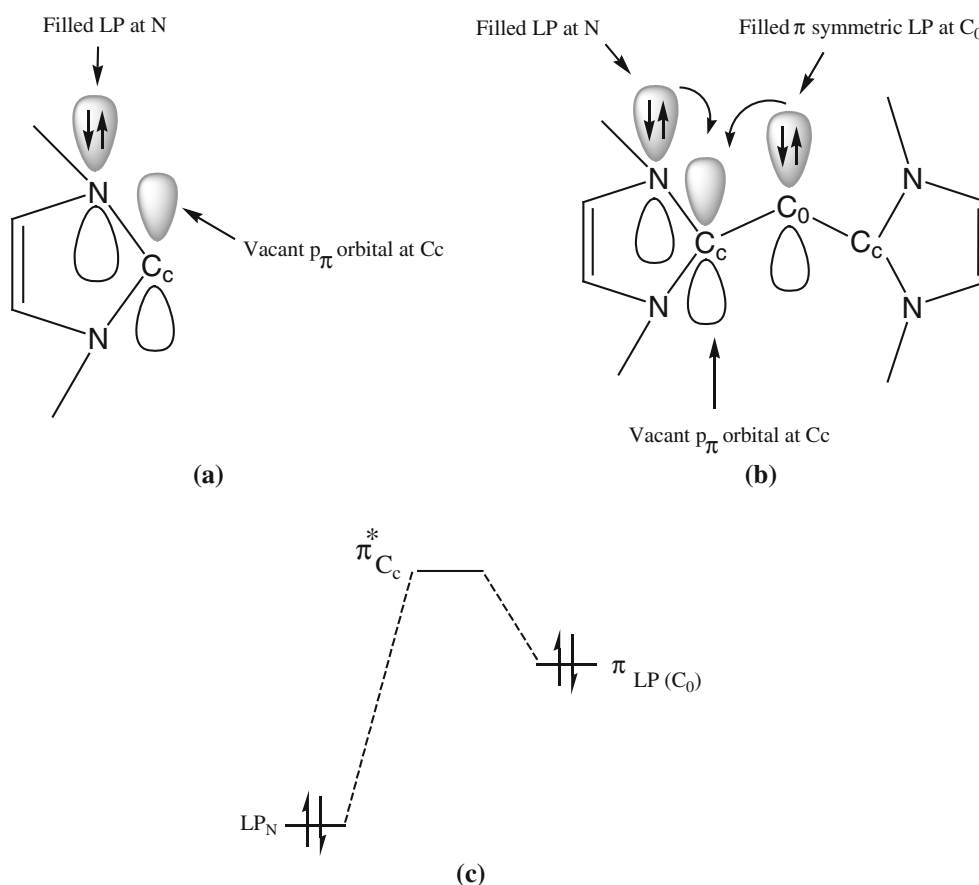
3H

3Me

3NH₂

3OH

3Cl

3F

5H

5Me

5NH₂

5OH

Fig. 2 Optimized geometries of the molecules calculated at BP86/TZVP level of theory

(a)

(b)

(c)

Scheme 3 Schematic representation of the possible orbital interactions in **a** free carbene, **b** carbodicarbene and **c** competition for the formally empty π symmetric orbital at the carbenic carbon (C_c) atom between the lone pair at N and the π symmetric lone pair at central C_0 atom
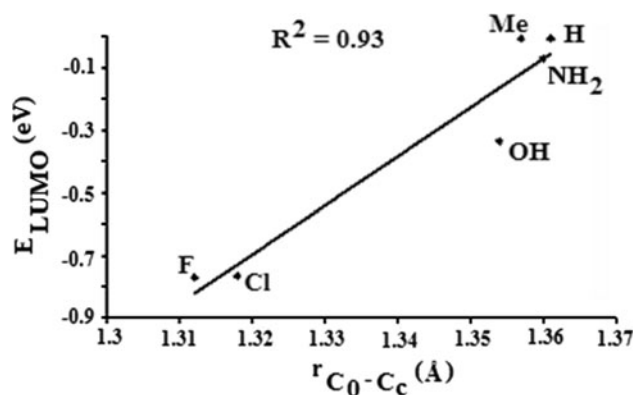

Fig. 3 Plot of the energy of the vacant P_π orbital on carbenic carbon (E_{LUMO}, eV) against the C_0–C_c bond lengths, $r(C_0$–$C_c)$ in Å

exhibit the characteristics of C(0)?" The energy differences between the equilibrium geometry and the geometry, where the central C_c–C_0–C_c angle of **3F** and **3Cl** is fixed at 130°, are only 7.6 and 4.1 kcal/mol, respectively. Thus, the bending potential of the C_c–C_0–C_c angle for these two compounds is not very deep compared to the parent allene $H_2C=C=CH_2$, which has an energy difference of 16.3 kcal/

mol between the equilibrium geometry and the geometry where the C–C–C angle were fixed at 136.9° [15]. Thus, this shallow bending potential and bonding analysis (vide infra) reveal that these two compounds have "masked" C(0) character.

All the optimized geometries (Fig. 2) of Si(NHC)$_2$ adopt a bent geometry at the central silicon atom like those of C(NHC)$_2$. The two NHC ligands are twisted with respect to the central C–Si–C plane by an angle that varies from 17.0 (**5H**) to 41.3° (**5Me**). Optimization of **5F** and **5Cl** leads to a structure in which two of the halogen atoms moved away from the nitrogen atoms of the two NHC ligands, and hence, these two structures were not considered for further discussion. There is no noticeable change in the Si_0–C_c bond lengths on changing the substituents attached to the N-atoms of the two NHCs (Fig. 2 and Table S2, supporting information). However, the Si_0–C_c bonds are weaker than those of C_0–C_c bonds as evident from the Wiberg Bond Index (WBI) values of the respective bonds (WBI values are indicative of the strength of a particular bond). This might be due to the fact that homopolar C_0–C_c bonds are stronger than heteropolar Si_0–C_c bonds (Fig. 2 and Table S1–S2). The C_c–N bonds of the free carbenes are stronger

than those of Si(0) compounds and is due to the same reason as given for C(0) compounds (vide supra). All the C_c–Si_0–C_c angles are typically close to 100° indicating that all these Si(0) compounds adopt a bent allene-type geometry. Unlike C(0) compounds, Si(0) compounds carry a positive charge at the central silicon atom except **5OH**. This might be due to lower electronegativity of silicon than carbon ($\chi_C = 2.5$, $\chi_{Si} = 1.9$) [40].

3.2 Natural bonding analysis

The bonding situations in **3** and **5** are thought to have a donor–acceptor type of interaction, L → E ← L (E = C, Si; L = NHCs) [13–19, 28]. This bonding situation results in the retention of two lone pairs at the central E(0) atom—one is of σ, and the other is of π symmetry. Interestingly, the default NBO calculations do not show any lone pair at the central carbon atom of **3**. This suggests that the most favorable Lewis structures of **3** should be written as $C_c=C_0=C_c$ rather than L → C ← L. Frenking et al. have

observed that enforcement of the σ and π symmetric lone pairs at the C_0 atom of $C(NHC)_2$ have a slightly higher residual density than that obtained by default NBO calculations [15]. Although the NBO calculations of **3** do not show any lone pair, a visual inspection of the frontier orbitals of **3** clearly shows that the C_0 atom has larger coefficients than the terminal atoms (Fig. 4). Figure 4 reveals that the HOMO and HOMO-1 of **3** are of π and σ symmetry, respectively. It is to be noted that the highest occupied molecular orbitals of **3F** and **3Cl** are energetically degenerate, which might be due to their quasi-linear geometries. Although the frontier orbitals of **3F** and **3Cl** are largely delocalized into the neighboring atoms, yet slightly larger coefficients are obtained at the C_0 atom.

The NBO calculations predict that the most favorable Lewis structure of **5** in its equilibrium geometry can be described by the donor–acceptor interaction, L → Si ← L. The percentage contribution of C_c and Si atoms for all the substituents attached to N-atoms of the NHCs are roughly 75 and 25, respectively, as evidenced from NBO analysis.

Fig. 4 Occupied frontier (HOMO and HOMO-1) orbitals of **3H**, **3F**, **3Cl**, and **5H**. Orbital energies are in eV

Molecule	HOMO	HOMO-1
3H	-3.26	-3.61
3Cl	-5.67	-5.67
3F	-6.19	-6.19
5H	-2.69	-4.39
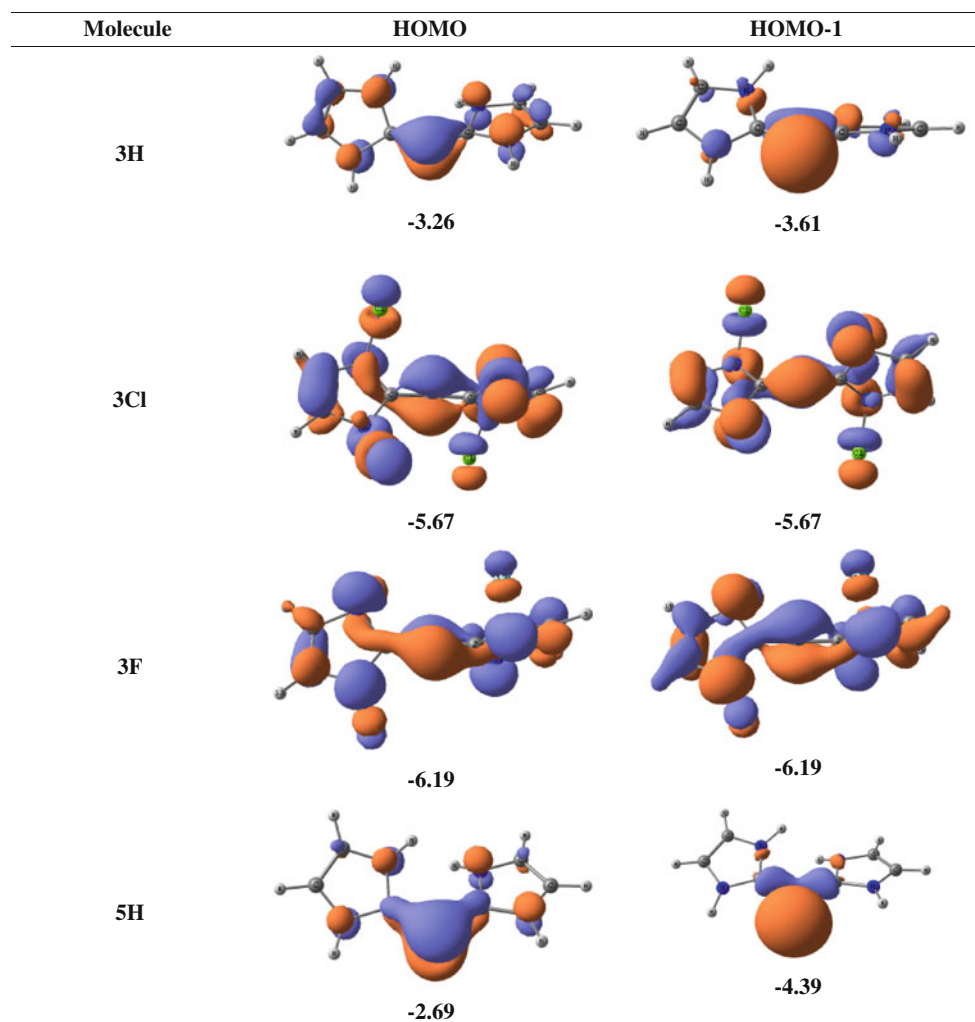
Thus, this donor–acceptor, $L \rightarrow Si \leftarrow L$, assertion is true for all the substituents considered in our study. Unlike in the case of carbodicarbenes **3**, NBO calculations of **5** clearly shows the presence of two lone pairs at the central silicon atom—one is of π symmetry (HOMO), and the other is of σ symmetry (HOMO-1). They are depicted in Fig. 4. It can be seen from Fig. 4 that the π symmetric lone pair is slightly delocalized toward the two carbenic carbon atoms.

3.3 QTAIM analysis

The bonding situations in **3** and **5** were further analyzed with quantum theory of atoms in molecules (QTAIM) [37, 38] to account for the differences in their equilibrium geometries. The theory embodies a natural partitioning of the molecular space into individual atomic basins. The surface bounding an atom in a molecule is one of zero flux in the gradient vector field of the electron density. A bond path is a line of maximum electron density connecting the two bonded atoms whose minimum lies at the bond critical point (BCP). A bond critical point is identified as three non-zero curvature of electron density (ρ_b), two of which are negative and is classified as (3, −1) critical point in ρ. The positive curvature λ_3 lies along the bond path, and the two negative curvature λ_1 and λ_2 lie perpendicular to it. The laplacian of the electron density at the bond critical point [$\nabla^2\rho$ (bcp)] is the summation of these three curvatures (or eigenvalues of the Hessian).

The compression of electron density perpendicular to the bond path results in negative values of λ_1 and λ_2, and its expansion along the bond path results in positive eigenvalue λ_3. Bader pointed out that these two competing processes decide the sign of the laplacian at the bond critical point. Generally, for covalent interactions (also referred to as "open-shell" or "sharing" interactions), ρ_b is large (>0.2 a.u), while $\nabla^2\rho$ (bcp) is large and negative. On the other hand, for closed-shell interactions (e.g., ionic, van der Waals', or hydrogen bonds), ρ_b is small (<0.10 a.u), and $\nabla^2\rho$ (bcp) is positive. But, a decision regarding the nature of a bond should not be made by considering the sign of the laplacian alone [37, 38, 44]. The local electronic energy density $H(r)$ is a valuable parameter for probing the nature of a bond. It is defined as the sum of local kinetic $G(r)$ and potential $V(r)$ energy density, that is, $H(r) = G(r) + V(r)$ [40]. Cremer and Kraka [44] proposed that a value of $H(r) < 0$ at BCPs presents a significant covalent contribution and accounts for the lowering of potential energy of electrons at BCPs. The magnitude of $H(r)$ reflects the "covalence" of interaction.

Figure 5 shows the laplacian plot of electron density in the C_c–E–C_c (E = C, Si) plane of **3H** and **5H**. The values of different topological parameters at the bond critical
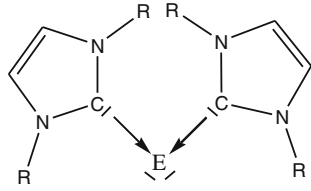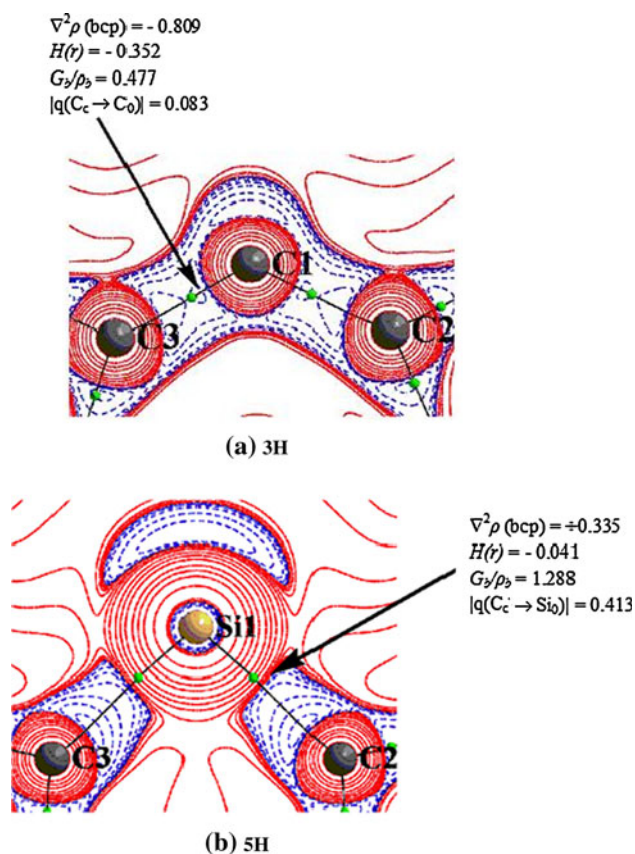

Fig. 5 Laplacian of electron density [$\nabla^2\rho$ *(bcp)*] in the C_c–E–C_c plane for **a 3H** and **b 5H**. *Solid red lines* represent charge depletion [$\nabla^2\rho$ (bcp) > 0], while *dashed blue lines* represent charge concentration [$\nabla^2\rho$ (bcp) < 0]. *Green dots* represent bond critical points. The values of laplacian, $\nabla^2\rho$ *(bcp)*, local energy density $H(r)$, relative kinetic energy density, G_b/ρ_b, and magnitude of charge transfer from carbenic carbon to E(0) atom (E = C of Si), $|q(C_c \rightarrow E_0)|$ are in atomic units

points of C_0–C_c and Si_0–C_c bonds are also provided in Fig. 5. It is evident from Fig. 5a that the bond between carbenic carbon and the central carbon is of shared type rather than a donor–acceptor one. The C_0–C_c bond critical point in **3** has very high negative value of laplacian $\nabla^2\rho$ *(bcp)* and local energy density $H(r)$, and a relative kinetic energy density (G_b/ρ_b) of less than 1. Further, there is very less charge transfer from C_c to C_0, $|q(C_c \rightarrow C_0)|$. Thus, all the values of different topological parameters [40] shown in Fig. 5a support the fact that the bonding situation in the equilibrium geometry of **3** should be described as $C_c{=}C_0{=}C_c$ rather than a dative interaction of the type $C_c \rightarrow C_0 \leftarrow C_c$. On the other hand, Fig. 5b reveals that the bond between carbenic carbon and the central silicon atom in **5** is of donor–acceptor type in which the carbenic carbon atoms act as the donor atoms and the central silicon atom acts as the acceptor atom. The Si_0–C_c bond in **5** has a small positive value of laplacian $\nabla^2\rho$ *(bcp)*, small negative value of local energy density $H(r)$, and has a relative kinetic

Table 1 Energy of the highest occupied π and σ symmetric lone pair orbitals [$E(LP_\pi)$ and $E(LP_\sigma)$ in eV], first(E_{PA-1}) and second (E_{PA-2}) proton affinities in kcal/mol calculated at the BP86/TZVP level of theory

Molecule	$E(LP_\pi)$	$E(LP_\sigma)$	E_{PA1}	E_{PA2}
3H	−3.26	−3.61	287.4	146.8
3Me	−3.17	−3.60	287.4	167.9
3NH$_2$	−3.64	−4.19	277.3	155.6
3OH	−4.22	−5.14	264.8	149.3
3Cl	−5.66	−5.66	256.0	146.2
3F	−6.19	−6.19	240.9	130.5
5H	−2.69	−4.39	274.2	169.3
5Me	−2.69	−4.13	277.9	179.7
5NH$_2$	−3.23	−4.76	266.0	177.8
5OH	−3.78	−5.42	256.6	171.9

The first proton affinity E_{PA-1} refers to the energy difference between the optimized geometries of the first protonated species and the parent molecule, while the second proton affinity E_{PA-2} refers to the energy difference between the optimized geometries of the second and the first protonated species

energy density (G_b/ρ_b) greater than 1. Moreover, the charge transfer from the carbenic carbon atom to the central silicon atom $|q(C_c \to Si_0)|$ is significant. Hence, all the topological properties shown in Fig. 5b further support the fact that the bonding situation in **5** in its equilibrium geometry should be described as $L \to Si \leftarrow L$.

3.4 Proton affinities

Since these $E(NHC)_2$ compounds are known to be highly basic in nature, we have decided to calculate their first and second proton affinities (Table 1). All the values of first and second proton affinities of **3** and **5** are significantly higher than the first (182.3 kcal/mol) and second (−2.8 kcal/mol) proton affinities of the parent allene $H_2C=C=CH_2$ calculated at the BP86/TZVP//BP86/SVP level of theory [14]. Interestingly, the values of the first and second proton affinities of **3F** and **3Cl** are higher than those

of the parent allene $H_2C=C=CH_2$. Thus, these higher values of proton affinities for **3F** and **3Cl** suggest that these two compounds have the characteristics of C(0) although it is "masked" in their respective equilibrium geometries. Further evidence came from the analysis of the natural charge at the central carbon atom in the first protonated species of **3F** and **3Cl**. The computed charge at the central carbon atom of **3F**–H$^{]+}$ and **3Cl**–H$^{]+}$ shows a high negative value of −0.376 and −0.450 units. This large increment in the negative charge (q_C = 0.061 and 0.045 for **3Cl** and **3F,** respectively, Fig. 2) at the central carbon atom of **3F**–H$^{]+}$ and **3Cl**–H$^{]+}$ is not due to simple electrostatic reason (there is a very small increment of negative charge at the central carbon atom of **3H**–H$^{]+}$ to **3OH**–H$^{]+}$). Rather, it is the donor–acceptor interaction that increases the negative charge at the C_0 atom of the protonated species. Hence, the characteristics of a C(0) compound imposed by the donor–acceptor type of interaction
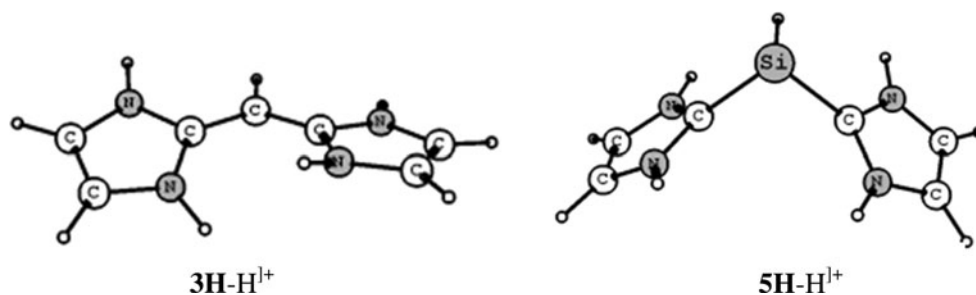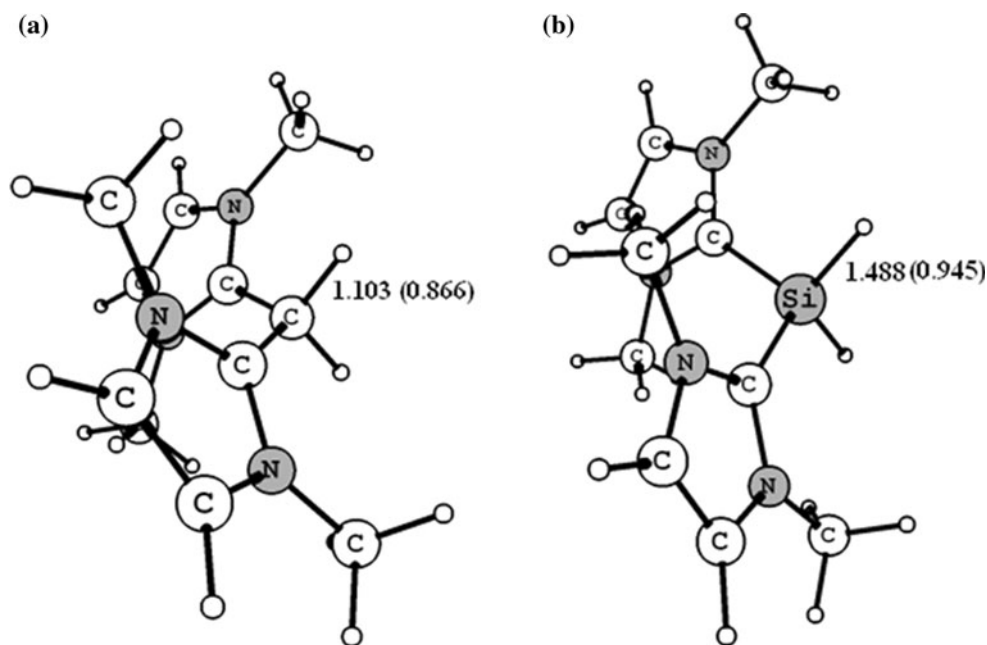
Fig. 6 Optimized geometries of the singly protonated E(0) species, **3H**-H$^{]+}$ and **5H**–H$^{]+}$

3H-H$^{]+}$

5H-H$^{]+}$

Fig. 7 Optimized geometries of the doubly protonated E(0) species **a** $C(0)–H_2^{]2+}$ and **b** $Si(0)–H_2^{]2+}$ (R = Me). $C(0)–$H and $Si(0)–$H bond lengths are in Å. Wiberg Bond Index (WBI) values of the respective bonds are shown in *parenthesis*

becomes prominent in describing the reactivity of **3F** and **3Cl** although it is "masked" in their equilibrium geometries. The masking of C(0) characteristics in their equilibrium geometries is due to the higher NHC–C(0) bond strengths of these two compounds. The $C_c–C_0$ bonds of **3F** and **3Cl** becomes so strong that their equilibrium geometries adopt a quasi-linear arrangement at the C_0 atom.

There is a distinct difference in the first protonation of $C(NHC)_2$ and $Si(NHC)_2$. In case of $C(NHC)_2$, the first protonation takes place at the σ symmetric lone pair, while the same takes place at the π symmetric lone pair for $Si(NHC)_2$. This is due to the fact that the energy separation between the σ and π symmetric lone pairs for $Si(NHC)_2$ is quite large compared to $C(NHC)_2$. Thus, the first protonation at the σ symmetric lone pair for $Si(NHC)_2$ will be energetically unfavorable. The cation **3**–H^{1+} has a planar arrangement around the central C_0 atom, while **5**–H^{1+} has a pyramidal arrangement around the central Si atom (Fig. 6), which further confirms that the first protonation of $C(NHC)_2$ and $Si(NHC)_2$ take place at the σ and π symmetric lone pairs, respectively. The first proton affinities of $Si(NHC)_2$ are smaller than those of $C(NHC)_2$. This might be due to the lower bond dissociation energies of Si–H compared to C–H bond [40].

The second protonation will take place at the σ-symmetric (HOMO) orbital of the first protonated species. Interestingly, the values of second proton affinities of $Si(NHC)_2$ are larger than $C(NHC)_2$. This might be due to the higher Si–H bond strengths in $Si(0)–H_2^{]2+}$ compared to C–H bond strengths in $C(0)–H_2^{]2+}$ (Fig. 7).

Figure 8a shows a nice correlation ($R^2 = 0.98$) between the energy of the σ symmetric lone pair of C(0) and the first
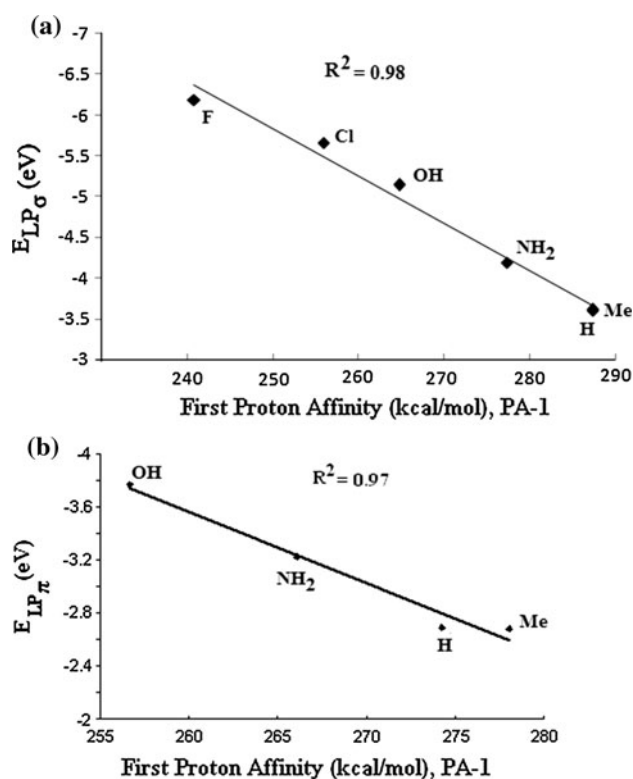

Fig. 8 Plots of (**a**) σ-symmetric lone pair of C(0) species against first proton affinities, PA-1 (kcal/mol) and (**b**) π-symmetric lone pair of Si(0) species against first proton affinities, PA-1 (kcal/mol)

proton affinity, while Fig. 8b shows a correlation ($R^2 = 0.97$) between the energy of the π symmetric lone pair of Si(0) with first proton affinity.

4 Conclusions

Quantum chemical calculations at BP86/TZVP level of theory have been performed on the carbon(0) and silicon(0) compounds where the two NHCs act as donor moieties, that is, NHC → E←NHC (E = C and Si). π donating and electron withdrawing substituents attached to N-atoms of the two NHCs not only affect the structures, but also their basicity. NHC–C(0) bond strengths were found to depend on the π accepting ability of the NHCs, that is, NHC–C(0) bond strengthens as the π accepting ability of NHCs increases. Substituents like F and Cl attached to N-atoms of the two NHCs in **3F** and **3Cl** result in quasi-linear allene geometry. These quasi-linear geometries in these two compounds "mask" the C(0) character in their equilibrium geometries. However, shallow bending potential of the central C_c–C_0–C_c angle of **3F** and **3Cl** and large negative natural charges at the central carbon atom of the protonated species **3F**–H$^{]+}$ and **3Cl**–H$^{]+}$ demonstrates that the equilibrium geometries of these two compounds have "hidden C(0) character," which becomes prominent in describing their reactivity. NBO calculations as well as atoms in molecules analysis suggest that the most favorable Lewis structure of the equilibrium geometries of C(NHC)$_2$ should be written as C_{NHC}=C=C_{NHC} rather than L → C ← L (L = NHCs). However, visual inspection of the frontier orbitals of C(NHC)$_2$ reveals that these compounds have two lone pairs with a higher coefficient at the central carbon atom. On the other hand, both NBO calculations and atoms in molecules analysis suggest that the most favorable Lewis structure of the equilibrium geometries of Si(NHC)$_2$ should be written as L → Si ← L (L = NHCs) and is true for all the substituents considered in our study. This striking difference between the equilibrium geometries of C(0) and its heavier group 14 analog, Si(0) is at par with the difference in the equilibrium geometries of acetylene and heavier group 14 analogs, E_2H_2 [41]. Moreover, electron withdrawing substituents attached to N-atoms of the two NHCs result in stabilization of the HOMO of these compounds, and as a result, their basicity decreases. The calculated first proton affinities of these compounds show a nice correlation with the energy of the corresponding orbital where protonation takes place. First proton affinities of C(0) compounds are higher than those of Si(0) compounds, while the second proton affinities of C(0) compounds are lower than that of Si(0) compounds.

We feel that the description of the bonding situations in **3** and **5** presented herein will be useful in predicting their E(0) characteristics. Since the discovery of carbon suboxide C(CO)$_2$ in 1906 [42, 43], numerous examples of main group elements stabilized by donor–acceptor interactions are now available, and it is expected that this versatile area of both theoretical and experimental research has a long future ahead.

References

1. Arduengo AJ, Harlow RL, Kline M (1991) J Am Chem Soc 113: 361–363
2. Herrmann WA (2002) Angew Chem Int Ed 41:1290–1309
3. Hahn FE, Jahnke MC (2008) Angew Chem Int Ed 47:3122–3172
4. Ramirez F, Desai NB, Hansen B, McKelvie N (1961) J Am Chem Soc 83:3539–3540
5. Hardy GE, Zink JI, Kaska WC, Baldwin JC (1978) J Am Chem Soc 100:8001–8002
6. Alcarazo M, Lehmann CW, Anoop A, Thiel W, Fürstner A (2009) Nat Chem 1:295–301
7. Alcarazo M (2011) Dalton Trans 40:1839–1845
8. Dyker CA, Lavallo V, Donnadieu B, Bertrand G (2008) Angew Chem Int Ed 47:3206–3209
9. Furstner A, Alcarazo M, Goddard R, Lehmann CW (2008) Angew Chem Int Ed 47:3210–3214
10. Kaska WC, Mitchell DK, Reichelderfer RF (1971) J Organomet Chem 47:391–402
11. Vicente J, Singhal AR, Jones PG (2002) Organometallics 21: 5887–5900
12. For the first synthesis of a *gem*-dimetallated carbodiphosphorane see: Schmidbaur H, Gasser O (1976) Angew Chem Int Ed 15: 501–502
13. Petz W, Kutschera C, Heitbaum M, Frenking G, Tonner R, Neumüller B (2005) Inorg Chem 44:1263–1274
14. Tonner R, Öxler F, Neumuller B, Petz W, Frenking G (2007) Angew Chem Int Ed 46:8695–8698
15. Tonner R, Frenking G (2008) Chem Eur J 14:3260–3272
16. Tonner R, Frenking G (2008) Chem Eur J 14:3273–3289
17. Tonner R, Frenking G (2009) Organometallics 28:3901–3905
18. Patil DS, Bharatam PV (2009) Chem Commun 1064–1066
19. Kaufhold O, Hahn FE (2008) Angew Chem Int Ed 47:4057–4061
20. Tonner R, Frenking G (2007) Angew Chem Int Ed 119:8850–8853
21. Viehe HG, Janousek Z, Gompper R, Lach D (1973) Angew Chem Int Ed 12:566–567
22. Oeser E (1974) Chem Ber 107:627–633
23. Janousek Z, Viehe HG (1971) Angew Chem Int Ed 10:574–575
24. Taylor MJ, Surman PWJ, Clark GR (1994) J. Chem Soc Chem Commun 2517–2518
25. Pinkerton AA, Schwarzenbach D (1978) J Chem Soc Dalton Trans 989–996
26. Patel DS, Bharatm PV (2011) J Org Chem 76:2558–2567
27. Ishida S, Iwamoto T, Kabuto C, Kira M (2003) Nature 421: 725–727
28. Takagi N, Shimizu T, Frenking G (2009) Chem Eur J 15: 3448–3456
29. Guha AK, Sarmah S, Phukan AK (2010) Dalton Trans 39: 7374–7383
30. Becke AD (1988) Phys Rev A 38:3098–3100
31. Perdew JP (1986) Phys Rev B 33:8822–8824
32. Schaefer A, Horn H, Ahlrichs R (1992) J Chem Phys 97: 2571–2577
33. Reed AE, Weinhold F (1983) J Chem Phys 78:4066–4073
34. Reed AE, Weinstock RB, Weinhold F (1985) J Chem Phys 83: 735–746

35. Reed AE, Curtiss LA, Weinhold F (1988) Chem Rev 88:899–926

36. Frisch MJ, Trucks GW, Schlegel HB, Scuseria GE, Robb MA, Cheeseman JR, Montgomery JA Jr, Vreven T, Kudin KN, Burant JC, Millam JM, Iyengar SS, Tomasi J, Barone V, Mennucci B, Cossi M, Scalmani G, Rega N, Petersson GA, Nakatsuji H, Hada M, Ehara M, Toyota K, Fukuda R, Hasegawa J, Ishida M, Nakajima T, Honda Y, Kitao O, Nakai H, Klene M, Li X, Knox JE, Hratchian HP, Cross JB, Bakken V, Adamo C, Jaramillo J, Gomperts R, Stratmann RE, Yazyev O, Austin AJ, Cammi R, Pomelli C, Ochterski JW, Ayala PY, Morokuma K, Voth GA, Salvador P, Dannenberg JJ, Zakrzewski VG, Dapprich S, Daniels AD, Strain MC, Farkas O, Malick DK, Rabuck AD, Raghavachari K, Foresman JB, Ortiz JV, Cui Q, Baboul AG, Clifford S, Cioslowski J, Stefanov BB, Liu G, Liashenko A, Piskorz P, Komaromi I, Martin RL, Fox DJ, Keith T, Al-Laham MA, Peng CY, Nanayakkara A, Challacombe M, Gill PMW, Johnson B, Chen W, Wong MW, Gonzalez C, Pople JA (2004) Gaussian 03, version D.01. Gaussian Inc., Wallingford CT

37. Bader RWF (1990) Atoms in molecules: a quantum theory. Oxford University Press, Oxford

38. Bader RFW (1991) Chem Rev 91:893–928

39. Keith T A (2010) AIMAll (Version 10.02.09) (http://aim.tkgristmill.com)

40. Huheey J E, Keiter E A, Keiter R L, Principles of Strucure and Reactivity, Fourth Edition, Pearson Education

41. Lein M, Krapp A, Frenking G (2005) J Am Chem Soc 127: 6290–6299

42. Diels O, Wolf B (1906) Ber Dtsch Chem Ges 39:689–697

43. For theoretical study on the equilibrium geometry of carbon suboxide see: Koput J (2000) Chem Phys Lett 320: 237–244

44. Cremer D, Kraka E (1984) Angew Chem Int Ed 23:627–628